

Visibility Reflects Dynamic Changes of Effective Connectivity between V1 and Fusiform Cortex

John-Dylan Haynes,^{1,3,4,*} Jon Driver,^{1,2} and Geraint Rees^{1,3}

¹Institute of Cognitive Neuroscience
University College London
Alexandra House
17 Queen Square
London WC1N 3AR
United Kingdom

²Department of Psychology
University College London
26 Bedford Way
London WC1H 0AP
United Kingdom

³Institute of Neurology
University College London
Queen Square
London WC1N 3BG
United Kingdom

⁴Department of Neurology II
Otto-von-Guericke-University
Leipziger Str. 44
D-39120 Magdeburg
Germany

Summary

Identifying the neural basis of visibility is central to understanding conscious visual perception. Visibility of basic features such as brightness is often thought to reflect activity in just early visual cortex. But here we show under metacontrast masking that fMRI activity in stimulus-driven areas of early visual cortex did not reflect parametric changes in the visibility of a brightness stimulus. The psychometric visibility function was instead correlated with activity in later visual regions plus parieto-frontal areas, and surprisingly, in representations of the unstimulated stimulus surround for primary visual cortex. Critically, decreased stimulus visibility was associated with a regionally-specific decoupling between early visual cortex and higher visual areas. This provides evidence that dynamic changes in effective connectivity can closely reflect visual perception.

Introduction

Understanding the neural determinants of visibility is crucial to understanding how visual awareness arises. Neurons at early stages of cortical processing are tuned to basic visual features such as brightness and contrast. Visibility of these properties might thus reflect activity in early visual cortex alone. Perceived brightness and contrast can correlate with activity in early, retinotopic visual cortex (Rossi et al., 1996; Boynton et al., 1999; Haynes et al., 2004). Moreover, activity in these areas can sometimes reflect the perceptual prop-

erties of a stimulus rather than its physical properties (e.g., Ress and Heeger, 2003; Haynes et al., 2003). This has led to suggestions that activity in early visual cortex may be necessary and sufficient for awareness of basic visual features (see Tong, 2003, and Rees et al., 2002, for reviews). But such proposals have typically been based on studies that only measured activity in early visual cortex and did not examine higher areas nor any functional coupling between early visual cortex and higher areas. Others have proposed that while activity in early visual cortex may be necessary, it is not sufficient for awareness without additional contributions from higher areas (see Crick and Koch, 1995). Later visual areas, plus parietal and prefrontal cortex, can show activity related to conscious detection of complex visual stimuli (e.g., faces or words; Lumer et al., 1998; Grill-Spector et al., 2000; Beck et al., 2001; Dehaene et al., 2001), but their role for perception of low-level stimuli has been rarely addressed. Furthermore, the potential role of functional coupling between regions in mediating visibility has only rarely been studied (Lumer and Rees, 1999).

Here, we investigated any role for coupling between early and higher visual areas in mediating visibility of low-level visual features, using a variant of the well-established perceptual phenomenon of *metacontrast masking* (reviewed in Breitmeyer and Ogmen, 2000). The visibility of a bright target stimulus can be substantially decreased if it is followed, after a brief delay, by a weak contour mask. The decrease in visibility depends critically on the exact timing between target and mask, with small changes in relative timing leading to large changes of visibility. Importantly, these visibility changes exhibit a characteristic U-shape when plotted as a function of stimulus-onset asynchrony (SOA; Breitmeyer and Ogmen, 2000). Such a nonmonotonic relationship between SOA and visibility can provide a very useful signature when assessing which brain regions may mediate changes in visibility, as regions where responses exhibit a simple linear (or other monotonic) correlation with SOA will not be confused with visibility-related areas. Metacontrast masking thus allows the study of visibility as a parametric graded function of SOA. Here, we used functional magnetic resonance imaging (fMRI) to test for neural responses in the human brain that followed the U-shaped psychophysical visibility function of each individual participant, and we examined in detail how activity changed in the retinotopic stimulus representations of early visual cortex. Importantly, we also examined whether the coupling between these cortical areas might reflect stimulus visibility, by measuring whether the strength of coupling, or effective connectivity (see Friston et al., 1997), between lower and higher areas was correlated with participants' visibility functions.

Besides the characteristic U-shaped psychometric profile, metacontrast masking has several further advantages for the present study. First, a weak outline mask can be sufficient to produce highly effective masking of a strong brightness stimulus. Second, the

*Correspondence: haynes@fil.ion.ucl.ac.uk

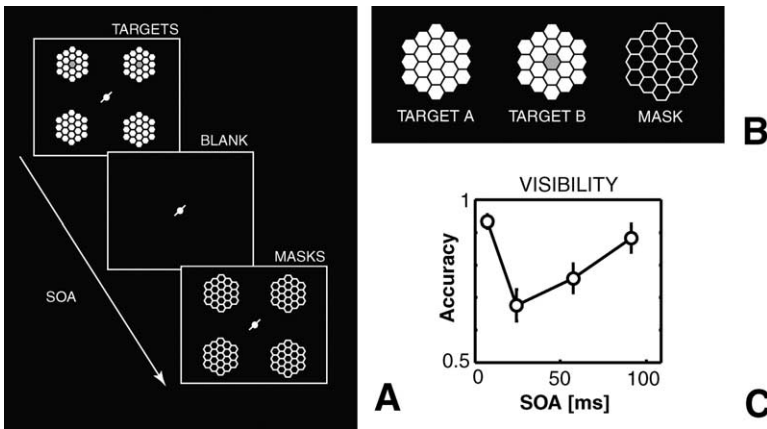


Figure 1. Stimulus Configuration and Psychophysical Results

(A) Temporal sequence of presentation. See [Experimental Procedures](#) for full details of timeline and stimuli and for advantages of these hexagonal stimuli.

(B) Enlarged versions of targets and masks (“target B” shows the target with a slightly darker center).

(C) Mean psychophysical accuracy of correct brightness discrimination (\pm SE) for the attended pair of stimuli on the cued diagonal as a function of target-mask SOA for eight subjects performing the task during fMRI scanning.

masking can affect perception of low-level features such as brightness, often thought to be represented in early visual cortex (Rossi et al., 1996; Haynes et al., 2004). Finally, metacontrast masking is traditionally thought to reflect processes within early visual cortex (Breitmeyer and Ogmen, 2000; Macknik and Livingstone, 1998), but may also be influenced by top-down modulation (Ramachandran and Cobb, 1995). Thus, it may provide an ideal paradigm for studying any possible coupling between lower and higher visual areas in mediating visibility.

To anticipate our findings, the psychometric visibility function was poorly correlated with activity in stimulus representations in retinotopic cortex; but strong correlations between activity and visibility were identified in higher visual areas V5/MT and the fusiform gyrus, in parietofrontal cortex, and surprisingly, also in representations of the unstimulated surround for primary visual cortex. Importantly, decreased stimulus visibility was reliably associated with a retinotopically and regionally specific decoupling between primary visual cortex and a focal region of fusiform cortex, as confirmed by several different analysis approaches.

Results

Psychometric Visibility

Participants maintained fixation on a central fixation mark while on each trial four composite target stimuli were presented briefly and simultaneously, one in each visual quadrant, followed after a brief delay (SOA) by four composite outline masks (Figure 1A). This quadrantic stimulus geometry allowed us to distinguish the activation produced by individual stimuli in retinotopic visual areas. The targets were bright white “honeycomb” patterns presented on a dark background, while the masks consisted of thin lines tracing the outer contours of these targets (see Figure 1B and [Experimental Procedures](#) for the advantages of using these honeycomb stimuli). A small central line instructed subjects to covertly attend to the two target stimuli in one diagonal pair of quadrants. In this way, we could also examine how attention might affect visual activations (cf. Ramachandran and Cobb, 1995), though this will not be

the main focus here. On each trial, one of the two stimuli on each diagonal (chosen randomly) had a slightly darker center (“target B” in Figure 1B) and participants had to indicate which one it was (for the attended diagonal) by using a button press with the right hand. This luminance discrimination served as an objective measure of visibility. As expected, subtle manipulations (jointly at all four locations) of the SOA between stimuli and subsequent masks produced the U-shaped visibility function that is characteristic of metacontrast masking (Figure 1C). There was a significant main effect of SOA on discrimination performance ($F_{3,28} = 5.2$; $p = 0.006$), and psychophysical discrimination during scanning was maximally impaired when the mask followed the target with a delay of 30–70 ms.

Whole-Brain Analyses

In order to identify any brain regions where the level of activity in the different conditions reflected the parametric changes in visibility, we first computed the “similarity” between the individual participants’ psychometric visibility functions and their brain responses (as a function of SOA). The Pearson correlation between each individual participant’s psychometric and neuro-metric profiles provided the objective measure of similarity and was computed separately for each voxel (see [Experimental Procedures](#), “whole-brain analysis”). This correlation was significant for only a small set of areas (Table 1). The fMRI signal from these areas, averaged across subjects, is plotted as a function of target-mask SOA in Figure 2A, confirming the similarity between these mean neurometric response profiles and the mean psychometric measure of stimulus visibility (cf. Figure 1C). The corresponding correlation coefficients are plotted in Figure 2C (“max. similarity”). The regions with significant psychometric-neurometric correlation were as follows: one region of retinotopic cortex, in the calcarine sulcus (CS); two areas of higher visual cortex (the fusiform gyrus and V5/MT+); plus four other areas including parietal and prefrontal cortex. Thus, only one region of early, retinotopic visual cortex, the CS, showed an activation pattern that reflected visibility during metacontrast masking. This is noteworthy given that such masking profoundly affects brightness per-

Table 1. Brain Areas with Significant Correlation to Psychophysics

X	Y	Z	Z Score	
15	-87	15	4.50	Calcarine sulcus (CS)
48	-45	-21	4.02	Fusiform gyrus (FG)
-45	-66	15	4.54	V5/MT+ (MT)
54	-63	15	4.02	V5/MT+ (MT)
-54	-48	27	3.83	Temporoparietal junction (TPJ)
-9	-63	33	4.44	Precuneus (PC)
3	-60	9	4.02	Posterior cingulate cortex (PCC)
-48	48	-6	3.83	Middle frontal gyrus (MFG)
-51	45	-3	4.02	Middle frontal gyrus (MFG)
30	15	45	4.02	Middle frontal gyrus (MFG)

Brain areas with a similarity measure (explained in [Experimental Procedures](#)) significantly larger than 0 (one sample t test, $df = 7$; $p_{\text{corr}} < 0.05$). X, Y, and Z are MNI standard coordinates (mm). These areas subsequently served as regions of interest for the analyses of functional coupling.

ception (see [Figure 1C](#)), which is often assumed to reflect activity in early visual cortex ([Rossi et al., 1996](#); [Haynes et al., 2004](#)). On the other hand, beyond retinotopic cortex there were several brain areas, including parietal and prefrontal cortex, that showed fMRI response profiles closely reflecting the U-shaped visibility profile.

Retinotopic Analyses of Early Visual Areas

The initial whole-brain fMRI analyses described above were performed after normalization of individual anatomy to standard space. However, stereotactic positions of early visual areas can be highly variable between subjects ([Amunts et al., 2000](#)). To examine early visual cortex more closely, we therefore undertook a more detailed analysis, identifying distinct retinotopic visual areas (V1, V2, V3, V3A, V4) within each individual using retinotopic mapping (cf. [Wandell, 1999](#); for details see [Experimental Procedures](#)). Due to the quadrantic specificity of retinotopic cortex, this also allowed us to distinguish brain activity related to the two currently attended versus two unattended stimuli. We found strong and reliable activation by the honeycomb stimulus in V1 through V4 that was also strongly modulated by attention ([Figure 2B](#)). But critically there was no U-shaped modulation reflecting visibility for these activations, not even in V1 (see the predominantly flat or monotonic SOA functions in [Figure 2B](#), with the slight dip for V4 not being reliable). This was also reflected in the lack of correlation between psychometric and neurometric profiles. The striking quadrantic specificity of the attention effects is also revealed by plotting the main effects of attention averaged across subjects on a standard brain template (see [Figure S5](#) in the [Supplemental Data](#) available online).

Center-Surround Organization of Responses in V1

The preceding retinotopic analysis raises an apparent paradox: stimulus-driven voxels in V1 showed no visibility-related profile in the retinotopic analysis ([Figure 2B](#)), yet a small region of visual cortex in the calcarine sulcus had shown such a U-shaped activity profile that correlated with visibility in the initial whole-brain analyses (top left of [Figure 2A](#)). These two findings can only be reconciled if they reflect activity from different sectors of primary visual cortex (note that the retinotopic analyses had been performed for *stimulus-driven* vox-

els in each visual area, whereas the whole-brain analysis was unrestricted). We inspected activation patterns for these different analyses on a computationally flattened representation of primary visual cortex for each participant ([Teo et al., 1997](#); [Wandell et al., 2000](#)). Remarkably, this revealed that sectors showing visibility-associated (i.e., U-shaped) profiles of activity in the calcarine sulcus were spatially distinct from the sectors of V1 directly responding to the stimulus, both in the group analysis of retinotopic cortex ([Figure 3](#)) and in individual participants ([Figure S4](#)). The cortical representation corresponding to the retinotopic location of the metacontrast stimuli responded strongly in a stimulus-driven manner (solid line in [Figure 3B](#), see also [Figure 3C](#)), but critically showed no modulation by mask SOA ([Figure 3E](#)). Visibility-associated activity (i.e., with a U-shaped SOA profile, [Figure 3F](#)) was instead confined to those regions of primary visual cortex representing the visual field immediately *surrounding* the metacontrast stimuli (dashed line in [Figure 3B](#), see also [Figure 3D](#)). Center and surround also differed in other functional profiles. In addition to being strongly stimulus-driven, the “center” sector (red arrow in [Figure 3B](#)) showed strong modulation by attention ([Figure 3E](#)), whereas the “surround” (green arrow in [Figure 3B](#)) showed weak attention effects ([Figure 3F](#)). Other retinotopic areas beyond V1 showed no evidence for this center-surround organization (see [Table S1](#)).

Effective Connectivity between Cortical Areas

The preceding analyses revealed a restricted set of cortical areas, both within visual cortex and beyond, whose responses correlated either with the psychometric visibility function or instead were strongly stimulus driven regardless of SOA. The finding that responses in several distinct areas may relate to visibility is intriguing. However, joint activation of areas is not sufficient to demonstrate any functional relationship between them. In order to gain insight into any functional relationship among this visibility-associated network, we next undertook an analysis of effective connectivity between these cortical areas.

Changes in effective connectivity between two brain regions can be studied by examining changes in covariation between their activities under different experimental conditions ([Friston et al., 1997](#); see [Experimental Procedures](#)). Such analyses are now well established not

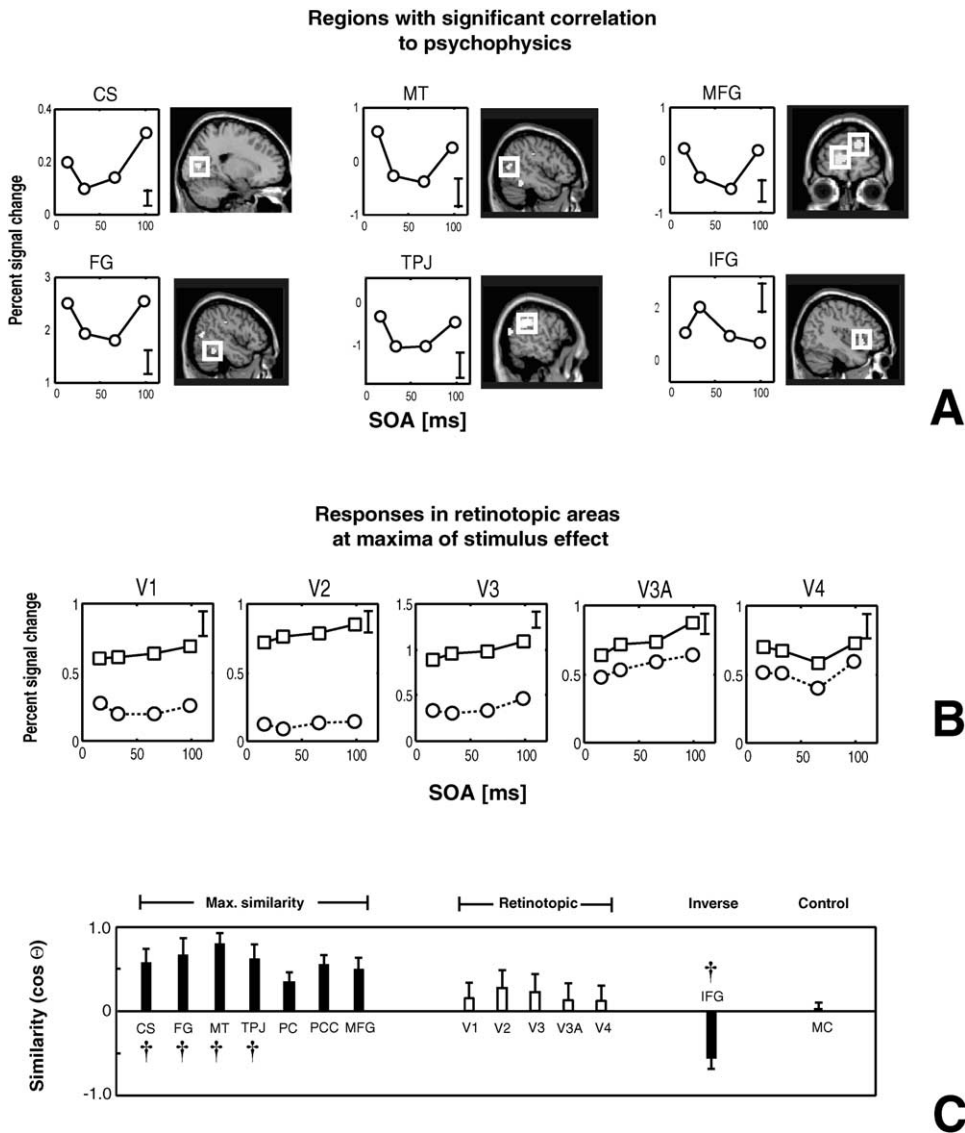


Figure 2. Brain Responses to Changing Target Visibility

(A) Normalized whole-brain analysis: BOLD signal changes (averaged across eight subjects) plotted as a function of target-mask SOA for cortical loci where responses significantly correlated with the individual participants' visibility functions ($p < 0.05$, corrected for multiple comparisons across voxels, error bars = SE). Area IFG was the only area showing a *negative* rather than positive correlation with visibility (at $p < 0.001$, uncorrected). In all of these areas there was a significant main effect of SOA ($df = 3,28$; all $p < 0.001$).

(B) BOLD responses for eight subjects plotted as in (A), but now for the maximally stimulus-driven voxels in retinotopic visual areas V1 through to V4 (attended quadrants = solid lines, squares; unattended quadrants = dashed lines, circles). Responses in all of these areas show a strong attention effect, but no U-shaped profiles reflecting visibility.

(C) Average correlation coefficients (across eight subjects) between profiles of brain responses and profiles of visibility (see [Experimental Procedures](#)). This correlation measures the "similarity" between U-shaped visibility functions of individual subjects and their BOLD signals in each particular brain area. Perfect similarity between BOLD signal and visibility profiles would be represented by a value of 1, no similarity by 0, and perfect similarity to the inverted response by -1 (black bars indicate significant correlation at $p < 0.05$; "CS" = calcarine activation found in the whole-brain analysis; "V1" activation in retinotopically defined area V1 at voxel maximally activated by the stimulus; IFG = inferior frontal gyrus; MC = left motor cortex, which served as a control area and shows no correlation; for other areas see [Table 1](#)). The daggers indicate regions where the mutual information between psychophysics and brain response is significantly larger than 0 ($p < 0.05$). This provides a nonparametric measure of similarity ([Steuer et al., 2002](#)) and confirms the results above, without assuming any linear relationship between visibility and brain response.

only for single neurons (e.g., [Aertsen et al., 1989](#)), but also for macroscopic signals from neuronal populations such as those recorded by EEG, MEG, and fMRI ([Gross et al., 2001](#); [Friston et al., 1997](#); [Macaluso et al., 2000](#);

[Stephan et al., 2003](#)). The strength of effective connectivity reflects the degree to which activity evoked in a neuronal population in one cortical area can be predicted by activity in another area, independently from

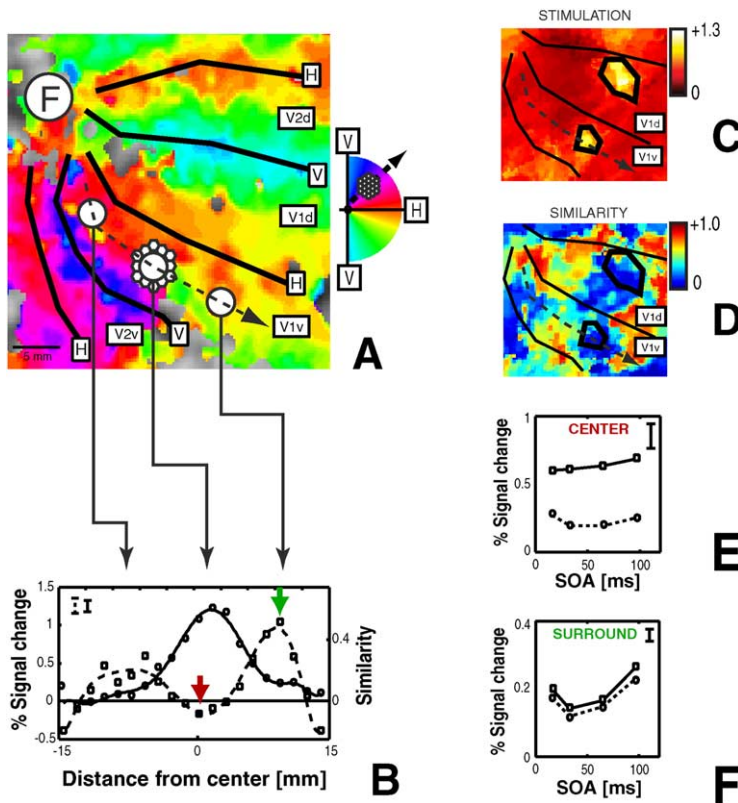


Figure 3. Center-Surround Organization of Stimulus Representation and Visibility-Related Activity in V1

(A) The phase angle of a rotating wedge stimulus is overlaid on a flattened representation of visual cortex (see Wandell, 1999, and Experimental Procedures) in the region of the calcarine sulcus (polar angle is coded as shown by the colormap). The graph also shows the position of the horizontal (“H”) and vertical (“V”) visual meridians and of the fovea (“F”). The dashed arrow indicates a cross-section through one quadrant of V1 from fovea to periphery corresponding to the cortical representation of one quadratic stimulus.

(B) Spatial distribution of stimulus-evoked activity (left axis, solid line) and similarity measure (right axis, dashed line) along the cross-section shown in (A) (averaged across subjects, error bars = SE). Remarkably, similarity reaches a peak in the surrounds of the stimulus-driven response (green arrow) and reaches a minimum in the retinotopic location of the stimulus itself (red arrow).

(C) and (D) show an example of this center-surround organization of stimulus-driven activity and similarity (V1 quadrant of one subject).

(E) and (F) show the mean responses (across subjects) for all four masking SOAs plotted separately for center (red arrow in [B]) and surround (green arrow in [B]) sectors of V1 and separately for attended (solid lines, squares) and unattended stimuli (dashed lines, circles, note the different scaling between [E] and [F]).

changes in correlation merely due to stimulus-locked transients evoked by sensory stimulation (Friston et al., 1997). Independence of overall activity within single areas versus coupling between areas is an important feature shared by all effective connectivity analyses (e.g., Friston et al., 1997; Gross et al., 2001; Aertsen et al., 1989; see Experimental Procedures). By estimating effective connectivity between areas in this way, we could characterize how it may change under different psychophysical contexts (in this case, the visibility of the stimulus as determined by the SOA).

To investigate whether psychophysical measures of visibility are reflected in the pattern of effective connectivity, we computed the correlation between all possible pair-wise combinations of areas that had shown visibility-associated responses (Table 1 and Figure 2A), plus all of the retinotopically mapped visual areas (including the stimulated and unstimulated sectors for V1), for each masking SOA. This broad initial selection of areas was undertaken deliberately in order not to be unduly restrictive (but as will be seen, the results were in fact highly selective). In order to avoid artifactual changes in correlation caused by a direct “driving” effect of the stimulus conditions, estimation of connectivity was performed using only the residuals after estimation and removal of the stimulus-driven effects (e.g., see Macaluso et al., 2000). We then identified those pairs of areas where the profile of changes in correlation (rather than the level of activity, as in the analyses presented earlier)

reflected the shape of individual participants’ psychometric functions (see Experimental Procedures and legend of Figure 4 for further details of this analysis). In accord with hypotheses that visibility may relate to functional coupling between early and higher visual cortex (e.g., Lamme and Roelfsema, 2000; Dehaene et al., 2003; Lumer and Rees, 1999), we found a highly regionally specific pattern of visibility-related modulation of the pattern of correlation (Figure 4) for V1 and the fusiform gyrus in particular. The similarity between these changes in correlation between areas and the psychophysical visibility function was significant for the coupling between V1 and fusiform gyrus, for both the stimulus-driven and the unstimulated surround sectors of V1 (asterisks in Figure 4C). Accordingly, these changes in correlation exhibited a U-shaped profile that reflected corresponding changes in visibility with SOA (Figure 4D). Such a relationship was observed both in this group analysis (Figure 4D) and in seven of the eight individual subjects (Figure S2).

To ensure that the visibility-related changes in correlation between V1 and FG indeed reflected changes in effective connectivity, we ruled out several alternate explanations. It is important to emphasize that visibility-related changes in correlation between areas did not simply reflect similar response profiles in each area. For example, the stimulus-driven regions of V1 and responses in FG showed very different activation profiles (see Figure 2), yet still showed a consistent change in

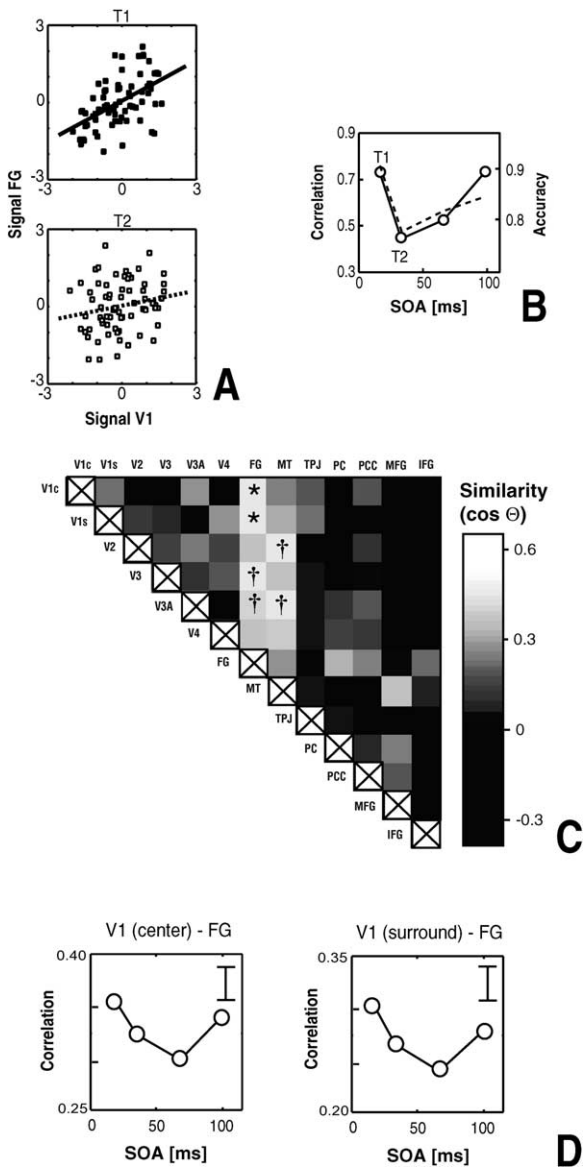


Figure 4. Dynamic Changes in Functional Coupling between Cortical Areas as a Function of Masking SOA

(A) The relationship between BOLD signals in two areas, stimulus driven sectors of primary visual cortex and fusiform gyrus (FG), is plotted for maximally visible (top, T1 = 16 ms SOA, filled symbols) and minimally visible stimuli (bottom, T2 = 33 ms SOA, open symbols; data for one illustrative subject; lines = regression slopes; each point represents BOLD signal from one image volume). It is apparent that the correlation between V1 and FG signal is reduced when stimulus visibility is reduced.

(B) Left axis: correlation between BOLD signals in V1 and FG as shown in (A), but now for all four target-mask SOAs (open circles, solid line). Right axis: psychophysical visibility data from the same subject (dashed line, note that the similarity measure we computed here between psychometric profile and profile of correlation is mean-corrected and thus independent of absolute scaling of the ordinate axis).

(C) Full coupling matrix. Each point in this matrix represents the mean value (across eight subjects) of the similarity between the psychometric visibility function (e.g., dashed line in [B]) and the change in correlation between those areas (e.g., solid line in [B]). This similarity metric is directly analogous to that plotted in Figure 2C, except that it is now calculated for the *functional coupling* between

their pattern of coupling that closely reflected visibility (Figure 4D). Moreover, the changes in correlation between pairs of areas were not related to a specific combination of main effects (e.g., one area showing a flat profile and one a U-shaped profile), because no other pair of areas with such overall activation profiles (e.g., other retinotopic areas, parietal and frontal regions) exhibited the same U-shaped profile of changes in coupling. Nor did this coupling result merely reflect anatomical proximity, as it was neither found between the stimulus and surround sectors of V1 themselves, nor among subsequent retinotopic visual areas (see Table S1). The result was also not caused by an increase in overall variability in the low-visibility conditions (e.g., due to any common top-down source of variability that might reflect the difficulty of detecting low versus high visibility stimuli, see Ress et al., 2000), since the overall level of variability itself in the fMRI signal was equivalent in V1 and FG in low- and high-visibility conditions (see Table S2). The coupling result was also unchanged when correct and incorrect responses were modeled as separate events to remove any variance due to differences between hit and miss responses (see Figure 4, caption). This means that potential differences between hits and misses in within-area response amplitudes are not the cause of our observed changes in coupling.

Finally, we confirmed that the regional specificity of the changes in connectivity we observed (i.e., between V1 and FG) had not arisen due to any bias in our preselection of cortical areas from our whole-brain and retinotopic analyses (which had been based on those areas identified in the earlier retinotopic and whole-brain analyses). An additional unconstrained whole-brain connectivity analysis revealed that the only areas throughout the brain to show significant ($p < 0.05$, corrected for multiple comparisons) visibility-associated coupling with primary visual cortex as a function of

areas rather than for overall activity within a single area (white = high similarity; V1c = V1 center; V1s = V1 surround). The asterisks indicate significant correlation between individual psychometric functions and functional coupling profiles ($p < 0.05$, Fisher-transformed and Bonferroni corrected). With a more lenient threshold ($p < 0.01$, uncorrected; daggers), further potential changes in functional coupling are revealed that show an apparently similar pattern (V3-FG, V3A-FG, V2-MT, V3A-MT), but these are not discussed further, given that they do not reach statistical significance at a corrected level.

(D) Changes in functional coupling between V1c and FG (left), and V1s and FG (right), as a function of SOA averaged across all subjects (error bars = SE). Note the U-shape of these changes in functional coupling. For both of these regions, the nonparametric measure of similarity (mutual information, see Steuer et al., 2002) between psychophysics and changes in connectivity is also significantly larger than 0 (V1c-FG, $p = 0.0007$; V1s-FG, $p = 0.0139$). An additional event-related analysis separately modeled the event-related activity associated with individual trial hits and misses and confirmed that functional coupling between V1 and FG (but not between other areas) was still highly correlated with individual subjects' psychometric visibility functions (V1c-FG, $r = 0.4152$, $p = 0.007$; V1s-FG, $r = 0.4278$, $p = 0.023$) even when this activity was removed. Please note that a separate analysis of coupling for hits versus misses is not possible, due to their event-related nature, unlike the blocked effects of functional coupling characterized here.

SOA were bilateral fusiform gyri (see [Figure S1](#)). Furthermore, the profile of changes in connectivity was not particular to the specific details of the analysis procedure employed, as a further analysis using a different method ([Friston et al., 2003](#)) for estimating effective connectivity resulted in the same findings of a U-shaped coupling profile ([Figure S3](#)). Taken together, these complementary analyses of effective connectivity using different analytic approaches all converge to show that our finding of a highly focal, visibility-related decrease in connectivity between V1 and fusiform gyrus was robust, generalizable across subjects, and anatomically highly specific.

Discussion

These data demonstrate that, in humans, visibility can be correlated with dynamic changes in effective connectivity *between* areas as revealed by fMRI. This significantly extends previous studies of visibility that had only measured activity *within* specific brain regions (e.g., [Bridgeman, 1975](#); [Bridgeman, 1980](#); [Green et al., 2005](#); [Kovács et al., 1995](#); [Lumer et al., 1998](#); [Macknik and Livingstone, 1998](#); [Rolls et al., 1999](#); [Grill-Spector et al., 2000](#); [Beck et al., 2001](#); [Dehaene et al., 2001](#); [Super et al., 2001](#); [Lamme et al., 2002](#); [Ress and Heeger, 2003](#)). Independently of the overall level of activity within an area, effective connectivity between areas showed patterns of modulation that directly related to participants' psychophysical functions against SOA (see [Figure 4](#) and [Figure S2](#) for individual subjects).

We observed that poor visibility was associated with a focal decoupling between primary visual cortex and the fusiform gyrus. This analysis of effective connectivity cannot determine whether the decoupling that we observed represented modulation of a feedforward or feedback signal. However, it is intriguing to note that a recent TMS study of metacontrast masking suggests that feedback signals to early visual cortex may play an important role in mediating visibility ([Ro et al., 2003](#)). Moreover, previous work has provided some suggestions that feedback signals may play a role in mediating visual awareness ([Lamme and Roelfsema, 2000](#); [Pasqual-Leone and Walsh, 2001](#); [Super et al., 2001](#)), although these electrophysiological studies have typically only recorded activity *within* a single area. (e.g., [Super et al., 2001](#); [Lamme et al., 2002](#)). Here we were able to exploit the ability of fMRI to concurrently measure activity throughout the whole brain in order to demonstrate that dynamic changes in the effective connectivity between specific areas (V1 and the fusiform gyrus) were correlated with visibility ([Figure 4](#) and [Figure S3](#)). Previously, visibility-related changes in effective connectivity between brain areas had been demonstrated with fMRI only for binary, categorical differences between perceptual states and without an online behavioral measure of perception ([Lumer and Rees, 1999](#)). In contrast, the present study measured brain signals and psychophysics concurrently. Moreover, our findings demonstrate that dynamic changes in effective connectivity can reflect graded parametric changes of visibility, as captured by relating the full psychometric profile to physiological functional coupling.

The brief nature of our stimuli and the masking procedure (that varied mask SOA over a few tens of milliseconds) are not inconsistent with our observation of a change in coupling between fMRI signals that vary more slowly. Not only do neural responses to brief stimuli typically extend for several hundred milliseconds, but neural signals associated with metacontrast masking can be observed well beyond the offset of the stimulus ([Bridgeman, 1975](#); [Bridgeman, 1980](#)). Such long-lasting visibility-associated signals have been previously proposed to represent the consequences of recurrent interactions between visual areas (see [Francis, 2000](#), for a review) that evolve over several hundred milliseconds. While the hemodynamic response measured using BOLD contrast fMRI evolves over several seconds, it is now well established that response latencies of a few hundred milliseconds or less can be resolved using such techniques ([Formisano and Goebel, 2003](#), for a review). Thus, very small differences in stimulus timing can evoke detectable changes in the BOLD signals, providing a plausible basis for our observations of visibility-dependent coupling between V1 and fusiform gyrus. The low-pass nature of the fMRI signal suggests that the functional coupling measured using this technique is likely to reflect correlated changes of macroscopic neural processing over a longer timescale (for example, the power of fluctuations of local field potentials in specific frequency band, see [Leopold et al., 2003](#)).

Previous studies investigating neural correlates of visual masking in the early visual cortex of cats and monkeys, with the very different method of single-cell electrophysiology, have produced somewhat variable results. Using the “standing wave of invisibility” paradigm ([Macknik and Livingstone, 1998](#); [Macknik and Haglund, 1999](#); [Macknik et al., 2000](#)), some effects of surround masking have been found in monkey V1. However, a recent study in humans showed that stimulus-driven regions of human V1 continued to carry information about the orientation of stimuli even though they were rendered completely invisible by such a standing wave of invisibility ([Haynes and Rees, 2005](#)). Unfortunately, because this paradigm combines forward and backward masking, it leaves unclear whether backward masking alone (as in the present paradigm) produces any response modulation in V1. In contrast, the few single-cell studies that specifically isolated backward masking typically found that backward masking did not affect early, transient stimulus-driven responses in V1 ([Bridgeman, 1975](#); [von der Heydt et al., 1997](#); [Macknik and Livingstone, 1998](#); [Lamme et al., 2002](#)). Rather than affecting the strong transient responses, effects of backward masking were typically relatively weak (when present) and restricted to late, low-amplitude stages of single-cell responses in V1, both for metacontrast paradigms similar to the present study (e.g., responses for SOAs between 0 and 500 ms in [Figure 4](#) of [Macknik and Livingstone, 1998](#)) and for pattern masking (e.g., [Figure 4](#) of [Lamme et al., 2002](#)). Similarly, metacontrast masking produced little or no modulation of early stimulus-driven components of the occipital ERP ([Vaughan and Silverstein, 1968](#)). The relatively late onset of response modulation in such paradigms has led to proposals that backward masking may be caused by some breakdown

of recurrent processing between early and later visual areas (Bridgeman, 1980; Lamme et al., 2002), consistent with the present demonstration of changes in functional coupling between V1 and fusiform gyrus reflecting changes in visibility.

We found a clear dissociation between *stimulus-driven* versus *surround* regions of primary visual cortex as to how closely the profile of responses as a function of SOA matched psychophysical visibility (Figure 3; Figure S4 for individual subject analyses; and Table S1 for specificity of response to V1). This echoes and extends recent reports of center-surround interactions in human visual cortex (Zenger-Landolt and Heeger, 2003; Shmuel et al., 2002; Smith et al., 2000; Muller and Kleinschmidt, 2004). A direct comparison is hindered by the very different paradigms used in each of these studies. However, the present findings are not compatible with surround suppression being invariably dependent on the degree of activation in stimulus-driven regions (e.g., Figure 5 in Shmuel et al., 2002). Instead, our unstimulated surround regions showed a U-shaped dependency on SOA, while the response amplitude in the stimulus-driven regions remained constant (Figure 3 and Figure S4 for individual subjects). The overall magnitude of unstimulated surround responses was weak compared to those in the stimulus-driven central regions (see Figure 3). One possibility is that visibility-associated responses were not seen in stimulus-driven regions due to saturation of the fMRI signal by strong stimulus-driven signals (e.g., due to the mask) and/or attentional signals. However, the responses to unattended stimuli did not reach ceiling (see Figure 2B) and yet still did not show a U-shaped response. Also, saturation cannot account for our finding of a visibility-associated signal in regions not directly driven by the stimulus. Our findings are strikingly consistent with recent observations that stimulus-driven regions of early visual cortex also fail to show effects of visibility when employing rather different overlapping masks that produce monotonic masking functions (Green et al., 2005), whereas ventral visual areas and certain parietal and prefrontal regions show weaker responses to masked than unmasked stimuli, similar to the present findings.

One intriguing possibility is that the unstimulated surround responses we observed may reflect signals that originate either through lateral connections with stimulus-driven sectors (Gilbert, 1992) or as a consequence of recurrent processing between V1 and other visual areas (Bridgeman, 1980; Lamme et al., 2002). In monkey, there are known anatomical connections between object-selective processing regions in temporal visual cortex and primary visual cortex (Rockland and Van Hoesen, 1994; Rockland et al., 1994). The functional homolog of such object-selective regions in humans includes the fusiform gyrus (Tanaka, 1997), thus providing a possible anatomical substrate for our new finding that the degree of functional coupling between fusiform gyrus and V1 reflected visibility. It is intriguing to note that in monkey, the back-projections from temporal cortex to V1 have a wider spread than feedback projections to extrastriate visual cortex (Rockland and Van Hoesen, 1994; Rockland et al., 1994). Thus, one possibility is that the visibility-related responses found in the stimulus-surround sectors of V1 may reflect relatively weak

modulation via such diffuse feedback connections, in the absence of conflicting direct bottom-up stimulus input that is itself not modulated by masking. However, such an interpretation has to await further research, as our measure of effective connectivity cannot directly distinguish between feedforward and feedback signals. It will therefore be important to establish in future studies whether the surround effects observed here play a functional role in mediating perception of the stimulus (cf. Ro et al., 2003).

Taken together, our results show that under conditions of metacontrast backward masking, activity in higher visually responsive areas (fusiform gyrus, V5/MT, and regions of parietal and prefrontal cortex) showed a better correlation with perception than did activity in stimulus-driven regions of early visual cortex. More generally, our findings show that although stimulus-driven activity in early visual cortex may be necessary for visibility of fundamental features such as brightness (Amassian et al., 1989; Horton and Hoyt, 1991), and in some cases can correlate closely with perception (Rossi et al., 1996; Ress and Heeger, 2003; Tong, 2003; Haynes et al., 2004), the level of activity in early areas alone may not always be sufficient to explain visibility (see also Rees et al., 2002). Critically, here visibility was also correlated with the extent of effective connectivity between early (V1) and later (fusiform gyrus) visual areas. Our results thus demonstrate that perception, even of low-level features such as brightness, can be associated with coupling between different levels of the visual system and also with activity in areas beyond traditional visual cortex (Crick and Koch, 1995; Lumer et al., 1998).

Conclusion

We used a metacontrast stimulus optimized for functional MRI in order to record responses throughout the brain associated with changes in stimulus visibility caused by metacontrast masking. While retinotopic regions of early visual cortex were primarily driven by the stimulus, responses specifically associated with visibility were seen in unstimulated surrounding sectors of V1, higher visual areas, and prefrontal and parietal cortex. Moreover, decreased visibility was associated with a highly focal decoupling between two of these areas: primary visual cortex and the fusiform gyrus. Our findings thus provide evidence that dynamic changes in effective connectivity can directly reflect visual perception.

Experimental Procedures

Stimuli and Experimental Design

Each target stimulus (see Figure 1) consisted of 19 small, filled hexagonal surfaces (diameter 0.8°, mean luminance 192 Cd/m²) arranged on a dark background (mean luminance 11 Cd/m²) in a honeycomb grid (spacing 0.05°). These “honeycomb” stimuli have several advantages when measuring brain activity with fMRI. First, they minimize the length of contour required to mask a given surface area while still allowing masking of a strong, bright target by a weak outline mask. Second, they enable a roughly isotropic tiling of an extended area of visual space while keeping the average distance between the contour and points on the target surface low. The mask stimuli consisted of a pattern of thin lines (0.05° diameter, mean luminance 192 Cd/m²) that filled the gaps and thus matched the outlines of the target stimuli. The four target/mask stimuli were

presented simultaneously in each of the four quadrants at an eccentricity of 7.5°. We organized the stimuli into visual quadrants to exploit the retinotopy of early visual areas. Visual stimuli were presented using an LCD projector with a frame rate of 60 Hz that projected onto a screen at the head-end of the scanner.

On each trial, first the four targets were presented simultaneously for 16.7 ms, followed by a variable interval of 16.7, 33.3, 66.7, or 100 ms, after which the masks were presented for 16.7 ms. During each scanning run, participants were required to maintain gaze on a central fixation spot. A small line cued the participants to attend covertly to the stimuli on one of the two diagonals (directing attention in this way to the diagonals encouraged stable fixation overall, although the display time of each stimulus was too short to permit saccadic eye movements). The central hexagon of one of the two stimuli on the attended diagonal was slightly darker (mean luminance 182 Cd/m²), and the participant had to indicate (in a two-alternative forced-choice task) which one by pressing one of two buttons of a response box. A randomly chosen stimulus on the unattended diagonal also had an identical brightness manipulation to avoid any stimulus-driven differences in brain activity between attended and unattended stimuli. Each block consisted of 15 trials (spaced by 1.5 s) with a constant masking SOA and a constant attended diagonal. During each run 16 such blocks were presented, which comprised two pseudorandomized sequences of the eight conditions (two attention conditions × four delay conditions) with fixation-only rest periods of 17.5 s inserted between each block. Before scanning, the subjects completed three to four runs of the same task outside the scanner to ensure they were able to perform the task and maintain stable fixation, as also confirmed by the retinotopic stimulus-driven activations we found.

fMRI Acquisition and Preprocessing

After giving informed consent, eight healthy volunteers (aged 22–33 years) participated. All had normal vision, were highly experienced with similar psychophysical tasks, and practiced the task prior to scanning. Data were acquired using a Siemens Allegra 3T scanner. For the main experiment, between five and six runs with 216 functional MRI volumes were collected per subject (48 slices; TR = 3.12 s; resolution 3 × 3 × 3 mm). A T1-weighted volume was acquired to allow coregistration of functional data with the individual subjects' structural scans. In a second session, we collected eight runs with 90 volumes of retinotopic mapping data for the same subjects. During these runs subjects viewed standard retinotopic mapping stimuli (Wandell, 1999) consisting of either wedges or rings that cyclically rotated or expanded with a phase duration of 31.2 s.

We analyzed fMRI data using SPM2 (<http://www.fil.ion.ucl.ac.uk/spm>). The first five images of each run were discarded to allow for magnetic saturation effects. The remaining images were realigned, resliced, coregistered to the individual subjects' structural scans, and (for the nonretinotopic analysis) spatially smoothed with a narrow Gaussian kernel of 5 mm full-width half-maximum. The data were high-pass filtered (cut-off frequency 0.0083 Hz) to remove low-frequency signal drifts and then subjected to two separate analyses, both using a voxel-wise general linear model (GLM) that included the eight experimental conditions and the motion correction parameters (as effects of no interest).

Whole-Brain Analyses

For the first (nonretinotopic) analysis, the individual subjects' functional scans were normalized to an MNI standard template prior to application of the GLM. The regression coefficients were collapsed across runs and attention conditions, resulting in four activation measures (one for each SOA) for each subject. The "similarity" between an individual subject's psychometric visibility function and the profile of brain responses was computed for each voxel as follows. The behavioral and brain response were each treated as a four-dimensional vector, where each entry corresponds to the measurement at one masking SOA. The mean of each vector was subtracted, resulting in two new vectors. The cosine of the angle between these two vectors is a measure of similarity that is independent of the scaling of the individual responses. It corresponds to the Pearson correlation coefficient. The resulting correlation

value for each subject and voxel was then Fisher-transformed and entered into a one sample t test ($p = 0.05$, corrected; see Figures 2A and 2C "max. similarity", and Table 1). Additionally, we also computed the mutual information between these two vectors (see Steuer et al., 2002) as a nonparametric measure of similarity that does not assume a linear relationship between visibility and neural response. These analyses were consistent with the results obtained using the Pearson correlation. Regions where the mutual information between psychophysics and neural response was significant ($p < 0.05$) are plotted in Figure 2C as daggers.

Retinotopic Analyses

The second analysis was based on individual subjects' retinotopic visual areas. To extract activity from individual regions in early visual cortex, we used 20 mask volumes for each region of interest (left and right V1d, V1v, V2d, V2v, V3d, V3v, plus the four quadrant representations of V3A and V4). These were obtained from the retinotopic mapping sessions following conventional methods (Wandell, 1999) and using Fourier analyses in SPM2 and segmentation and cortical flattening in MrGray (<http://white.stanford.edu/~brian/mri/segmentUnfold.htm>). In each of these regions of interest, we then chose the maxima for activation by metacontrast stimuli and extracted the average response (regression coefficients averaged across runs). The average responses for each subject and condition were then used to plot Figure 2B. For all retinotopic areas, there was a significant main effect of attention but no significant interactions between attention and target-mask SOA. The correlations between neurometric and psychometric profiles were computed as above and are also plotted in Figure 2C ("retinotopic").

Topographical Analysis of Similarity Measure in V1

In order to analyze the spatial distribution of stimulus-driven effects and similarity effects within retinotopically mapped V1, the regressors for the main effect of stimulation and the similarity measure were overlaid on computationally flattened representations of individual subjects' occipital cortex (Teo et al., 1997; Wandell et al., 2000; e.g., Figures 3C and 3D). To obtain an average profile of these measures across all subjects (Figure 3B), a 30 mm cross-section was taken that followed the gradient of eccentricity from the fovea to the periphery and ran in the middle between the representations of horizontal and vertical meridians in V1 (see dashed arrows in Figure 3A). This corresponds to the location of the quadrant stimuli. The topographic profiles in individual subjects, which are highly consistent, are shown in Figure S4.

Effective Connectivity

The analysis of effective connectivity was initially performed using an extension of an established fMRI analysis method (Macaluso et al., 2000; Stephan et al., 2003) for identifying "psychophysiological interactions." This extension was implemented to facilitate computation of the entire connectivity matrix shown in Figure 4C and critically to test for dynamic changes in functional coupling in relation to psychophysical performance (and hence visibility) at the four mask SOAs. In order to avoid artifactual changes in functional coupling caused by a direct "driving" effect of the stimulus conditions, estimation of functional coupling was performed using the residuals after estimation and removal of the stimulus-driven effects (Macaluso et al., 2000). First, the time courses of the residuals were extracted from the voxels in early visual areas showing a maximum stimulation effect (for V1c, V2, V3, V3A, V4) and from the voxels with maximum correlation with the visibility function (for V1s, FG, MT, PCC, PC, TPJ, MFG, IFG). The residuals were obtained by first estimating the full GLM (as for the whole-brain analyses) with separate regressors for each SOA and for subject motion. Then a characteristic regional time course of the residuals (i.e., the variance not accounted for by this model) was extracted from the selected voxels. Only the residuals were used in order to ensure that any changes in correlation between different masking SOAs could not simply be due to differences in the main responses to stimulation or to movement-related artifacts. Note that the residuals had similar variance across all conditions (see Table S2), ruling out the possibility that nonspecific contributions to residual variance (e.g., possible top-down effects that might differ under different visibility

conditions; [Rees et al., 2000](#)) might contribute to our coupling measurements. The correlation between these residual time courses was then computed for each pair of areas separately, for each of the four target-mask delays. The similarity measure between individual neurometric and psychometric profiles was then computed as above, but now between the profiles of changes in functional coupling and the profiles of psychophysical visibility against SOA (an example is shown in [Figure 4B](#), and the individual subject profiles for every subject are shown in [Figure S2](#)). Overall, this procedure allowed dynamic changes in functional coupling between areas to be revealed that depended solely on the psychophysical visibility of the stimuli as a function of masking SOA.

Further analyses of effective connectivity using an unconstrained “psychophysiological interaction” approach ([Friston et al., 1997](#)) and a more detailed computational model ([Friston et al., 2003](#)) are presented in the [Supplemental Data](#) (as [Figures S1](#) and [S3](#)), to show that our findings are not specific to any one analysis approach. Finally, further analyses of effective connectivity where variance potentially associated with correctly versus incorrectly perceived events is modeled and removed are also presented in the [Supplemental Data](#) (as [Figure S5](#)).

Supplemental Data

The Supplemental Data for this article can be found at <http://www.neuron.org/cgi/content/full/46/5/811/DC1>.

Acknowledgments

The Wellcome Trust and the BBSRC (UK) supported this work. We thank Evelyn Eger, Elliot Freeman, Klaas Enno Stephan, and four anonymous reviewers for helpful comments on the paper.

Received: June 11, 2004

Revised: November 19, 2004

Accepted: May 6, 2005

Published: June 1, 2005

References

- Aertsen, A.M.H.J., Gerstein, G.L., Habib, M.K., and Palm, G. (1989). Dynamics of neural firing correlation: modulation of “effective connectivity”. *J. Neurophysiol.* **61**, 900–917.
- Amassian, V.E., Cracco, R.Q., Maccabee, P.J., Cracco, J.B., Rudell, A., and Eberle, L. (1989). Suppression of visual perception by magnetic coil stimulation of human occipital cortex. *Electroencephalogr. Clin. Neurophysiol.* **74**, 458–462.
- Amunts, K., Malikovic, A., Mohlberg, H., Schormann, T., and Zilles, K. (2000). Brodmann’s areas 17 and 18 brought into stereotaxic space—where and how variable? *Neuroimage* **11**, 66–84.
- Beck, D.M., Rees, G., Frith, C.D., and Lavie, N. (2001). Neural correlates of change detection and change blindness. *Nat. Neurosci.* **4**, 645–650.
- Boynton, G.M., Demb, J.B., Glover, J.H., and Heeger, D.H. (1999). Neuronal basis of contrast discrimination. *Vision Res.* **39**, 257–269.
- Breitmeyer, B.G., and Ogmen, H. (2000). Recent models and findings in visual backward masking: a comparison, review, and update. *Percept. Psychophys.* **62**, 1572–1595.
- Bridgeman, B. (1975). Correlates of metacontrast in single cells of the cat visual system. *Vision Res.* **15**, 91–99.
- Bridgeman, B. (1980). Temporal response characteristics of cells in monkey striate cortex measured with metacontrast masking and brightness discrimination. *Brain Res.* **196**, 347–364.
- Crick, F., and Koch, C. (1995). Are we aware of neural activity in primary visual cortex? *Nature* **375**, 121–123.
- Dehaene, S., Naccache, L., Cohen, L., Bihan, D.L., Mangin, J.F., Poline, J.B., and Riviere, D. (2001). Cerebral mechanisms of word masking and unconscious repetition priming. *Nat. Neurosci.* **4**, 752–758.
- Dehaene, S., Sergent, C., and Changeux, J.P. (2003). A neuronal network model linking subjective reports and objective physiological data during conscious perception. *Proc. Natl. Acad. Sci. USA* **100**, 8520–8525.
- Formisano, E., and Goebel, R. (2003). Tracking cognitive processes with functional MRI mental chronometry. *Curr. Opin. Neurobiol.* **13**, 174–181.
- Francis, G. (2000). Quantitative theories of metacontrast masking. *Psychol. Rev.* **107**, 768–785.
- Friston, K.J., Buechel, C., Fink, G.R., Morris, J., Rolls, E., and Dolan, R.J. (1997). Psychophysiological and modulatory interactions in neuroimaging. *Neuroimage* **6**, 218–229.
- Friston, K.J., Harrison, L., and Penny, W. (2003). Dynamic causal modeling. *Neuroimage* **9**, 1273–1302.
- Gilbert, C.D. (1992). Horizontal integration and cortical dynamics. *Neuron* **9**, 1–13.
- Green, M.F., Glahn, D., Engel, S.A., Nuechterlein, K.H., Sabb, F., Strojwas, M., and Cohen, M.S. (2005). Regional brain activity associated with visual backward masking. *J. Cogn. Neurosci.* **17**, 13–23.
- Grill-Spector, K., Kushnir, T., Hendler, T., and Malach, R. (2000). The dynamics of object-selective activation correlate with recognition performance in humans. *Nat. Neurosci.* **3**, 837–843.
- Gross, J., Kujala, J., Hamalainen, M., Timmermann, L., Schnitzler, A., and Salmelin, R. (2001). Dynamic imaging of coherent sources: Studying neural interactions in the human brain. *Proc. Natl. Acad. Sci. USA* **98**, 694–699.
- Haynes, J.D., and Rees, G. (2005). Predicting the orientation of invisible stimuli from activity in human primary visual cortex. *Nat. Neurosci.* **8**, 686–691.
- Haynes, J.D., Roth, G., Stadler, M., and Heinze, H.J. (2003). Neuro-magnetic correlates of perceived contrast in primary visual cortex. *J. Neurophysiol.* **89**, 2655–2666.
- Haynes, J.D., Lotto, R.B., and Rees, G. (2004). Responses of human visual cortex to uniform surfaces. *Proc. Natl. Acad. Sci. USA* **101**, 4286–4291.
- Horton, J.C., and Hoyt, W.F. (1991). The representation of the visual field in human striate cortex. A revision of the classic Holmes map. *Arch. Ophthalmol.* **109**, 816–824.
- Kovács, G., Vogels, R., and Orban, G. (1995). Cortical correlate of pattern backward masking. *Proc. Natl. Acad. Sci. USA* **92**, 5587–5591.
- Lamme, V.A., and Roelfsema, P.R. (2000). The distinct modes of vision offered by feedforward and recurrent processing. *Trends Neurosci.* **23**, 571–579.
- Lamme, V.A., Zipser, K., and Spekreijse, H. (2002). Masking interrupts figure-ground signals in V1. *J. Cogn. Neurosci.* **14**, 1044–1053.
- Leopold, D., Murayama, Y., and Logothetis, N.K. (2003). Very slow activity fluctuations in monkey visual cortex: Implications for functional brain imaging. *Cereb. Cortex* **13**, 422–433.
- Lumer, E.D., and Rees, G. (1999). Covariation of activity in visual and prefrontal cortex associated with subjective visual perception. *Proc. Natl. Acad. Sci. USA* **96**, 1669–1673.
- Lumer, E.D., Friston, K.J., and Rees, G. (1998). Neural correlates of perceptual rivalry in the human brain. *Science* **280**, 1930–1934.
- Macaluso, E., Frith, C.D., and Driver, J. (2000). Modulation of human visual cortex by crossmodal spatial attention. *Science* **289**, 1206–1208.
- Macknik, S.L., and Haglund, M.M. (1999). Optical images of visible and invisible percepts in the primary visual cortex of primates. *Proc. Natl. Acad. Sci. USA* **96**, 15208–15210.
- Macknik, S.L., and Livingstone, M.S. (1998). Neuronal correlates of visibility and invisibility in the primate visual system. *Nat. Neurosci.* **1**, 144–149.
- Macknik, S.L., Martinez-Conde, S., and Haglund, M.M. (2000). The role of spatiotemporal edges in visibility and visual masking. *Proc. Natl. Acad. Sci. USA* **97**, 7556–7560.
- Muller, N.G., and Kleinschmidt, A. (2004). The attentional ‘spot-

- light's penumbra: center-surround modulation in striate cortex. *Neuroreport* 15, 977–980.
- Pascual-Leone, A., and Walsh, V. (2001). Fast backprojections from the motion to the primary visual area necessary for visual awareness. *Science* 292, 510–512.
- Ramachandran, V.S., and Cobb, S. (1995). Visual attention modulates metacontrast masking. *Nature* 373, 66–68.
- Ress, D., and Heeger, D.J. (2003). Neuronal correlates of perception in early visual cortex. *Nat. Neurosci.* 6, 414–420.
- Ress, D., Backus, B.T., and Heeger, D.J. (2000). Activity in primary visual cortex predicts performance in a visual detection task. *Nat. Neurosci.* 3, 940–945.
- Rees, G., Kreiman, G., and Koch, C. (2002). Neural correlates of consciousness in humans. *Nat. Rev. Neurosci.* 3, 261–270.
- Ro, T., Breitmeyer, B., Burton, P., Singhal, N.S., and Lane, D. (2003). Feedback contributions to visual awareness in human occipital cortex. *Curr. Biol.* 13, 1038–1041.
- Rockland, K.S., and Van Hoesen, G.W. (1994). Direct temporal-occipital feedback connections to striate cortex (V1) in the macaque monkey. *Cereb. Cortex* 4, 300–313.
- Rockland, K.S., Saleem, K.S., and Tanaka, K. (1994). Divergent feedback connections from areas V4 and TEO in the macaque. *Vis. Neurosci.* 11, 579–600.
- Rolls, E.T., Tovéé, M.J., and Panzeri, S. (1999). The neurophysiology of backward visual masking: Information analysis. *J. Cogn. Neurosci.* 11, 300–311.
- Rossi, A.F., Rittenhouse, C.D., and Paradiso, M.A. (1996). The representation of brightness in primary visual cortex. *Science* 273, 1104–1107.
- Shmuel, A., Yacoub, E., Pfeuffer, J., Van de Moortele, P.F., Adriany, G., Hu, X., and Ugurbil, K. (2002). Sustained negative BOLD, blood flow and oxygen consumption response and its coupling to the positive response in the human brain. *Neuron* 36, 1195–1210.
- Smith, A.T., Singh, K.D., and Greenlee, M.W. (2000). Attentional suppression of activity in the human visual cortex. *Neuroreport* 11, 271–277.
- Stephan, K.E., Marshall, J.C., Friston, K.J., Rowe, J.B., Ritzl, A., Zilles, K., and Fink, G.R. (2003). Lateralized cognitive processes and lateralized task control in the human brain. *Science* 301, 384–386.
- Steuer, R., Kurths, J., Daub, C.O., Weise, J., and Selbig, J. (2002). The mutual information: Detecting and evaluating dependencies between variables. *Bioinformatics* 18, S231–S240.
- Super, H., Spekreijse, H., and Lamme, V.A. (2001). Two distinct modes of sensory processing observed in monkey primary visual cortex (V1). *Nat. Neurosci.* 4, 304–310.
- Tanaka, K. (1997). Mechanisms of visual object recognition: monkey and human studies. *Curr. Opin. Neurobiol.* 7, 523–529.
- Teo, P.C., Sapiro, G., and Wandell, B.A. (1997). Creating connected representations of cortical gray matter for functional MRI visualization. *IEEE Trans. Med. Imaging* 16, 852–863.
- Tong, F. (2003). Primary visual cortex and visual awareness. *Nat. Rev. Neurosci.* 4, 219–229.
- Vaughan, H.G., and Silverstein, L. (1968). Metacontrast and evoked potentials: a reappraisal. *Science* 160, 207–208.
- von der Heydt, R., Friedman, H.S., Zhou, H., Komatsu, H., Hanzawa, A., and Murakami, I. (1997). Neuronal responses in monkey V1 and V2 unaffected by metacontrast. *Invest. Ophthalmol. Vis. Sci.* 38 (suppl.), 2146.
- Wandell, B.A. (1999). Computational neuroimaging of human visual cortex. *Annu. Rev. Neurosci.* 22, 145–173.
- Wandell, B.A., Chial, S., and Backus, B. (2000). Visualisation and measurement of the cortical surface. *J. Cogn. Neurosci.* 12, 739–752.
- Zenger-Landolt, B., and Heeger, D.J. (2003). Response suppression in V1 agrees with psychophysics of surround masking. *J. Neurosci.* 23, 6884–6893.